

A Wigner Surmise for Hermitian and Non-Hermitian Chiral Random Matrices

G. Akemann[‡], E. Bittner[‡], M.J. Phillips[‡], and L. Shifrin[‡]

[‡]*Department of Mathematical Sciences & BURSt Research Centre,
Brunel University West London, Uxbridge UB8 3PH, United Kingdom*

[‡]*Institute for Theoretical Physics and Centre for Theoretical Sciences (NTZ),
University Leipzig, P.O. Box 100 920, D-04009 Leipzig, Germany*

(Dated: September 10, 2018)

We use the idea of a Wigner surmise to compute approximate distributions of the first eigenvalue in chiral Random Matrix Theory, for both real and complex eigenvalues. Testing against known results for zero and maximal non-Hermiticity in the microscopic large- N limit we find an excellent agreement, valid for a small number of exact zero-eigenvalues. New compact expressions are derived for real eigenvalues in the orthogonal and symplectic classes, and at intermediate non-Hermiticity for the unitary and symplectic classes. Such individual Dirac eigenvalue distributions are a useful tool in Lattice Gauge Theory and we illustrate this by showing that our new results can describe data from two-colour QCD simulations with chemical potential in the symplectic class.

PACS numbers: 02.10.Yn,12.38.Gc

1. *Motivation.* Probably one of the most used predictions of Random Matrix Theory (RMT) is the so-called Wigner surmise (WS) describing the universal repulsion of energy levels in many systems in nature, including neutron scattering, quantum billiards and elastomechanical modes in crystals [1]. For large matrices, the nearest-neighbour (nn) spacing distribution $p^{(\beta)}(s)$ is universal and only depends on the repulsion strength which takes discrete values $\beta = 1, 2, 4$ for the three classical Wigner-Dyson (WD) ensembles. It can be computed with surprising accuracy using 2×2 matrices, which is the WS. Although simple arguments discussed in [2] lead to this rule for $\beta = 1$, such an approximation is by no means obvious.

The extension from WD to non-Hermitian RMT introduced long ago by Ginibre [3] has become a very active field in the past decade, in particular due to applications in open quantum systems, see [4] for references and other applications. Here the spacing is known only for the class with broken time-reversal ($\beta = 2$) and has been applied in Lattice Gauge Theory (LGT) [5]. However, a simple surmise based on 2×2 matrices does not work here.

In this paper we investigate the existence of a surmise for the smallest eigenvalue in chiral RMT and its non-Hermitian extensions. These have become relevant due to applications in Quantum Chromodynamics (QCD) initiated by [6] and extended to non-Hermitian QCD at finite quark chemical potential μ [7]. QCD at strong coupling is a notoriously difficult theory, and the chiral RMT approach has become an important tool for LGT with exact chiral fermions [8, 9]. For non-Hermitian QCD the complex action hampers a straightforward LGT approach, see [10] for a recent discussion and references. Here RMT predictions remain possible for various quantities [11, 12, 13].

In this paper we will show that an excellent approximation for the 1st non-zero eigenvalue is possible using a simple $2 \times (2 + \nu)$ matrix calculation, capturing the

repulsion of a small number ν of zero eigenvalues. Being localised and non-oscillatory the 1st eigenvalue is much more suitable for LGT than the spectral density, compare e.g. [9] and [14]. Our surmise fills some gaps in predictions for real eigenvalues in the orthogonal and symplectic classes ($\beta = 1, 4$) [15], where until very recently numerically generated RMT had to be used for comparison [16]. We also provide new predictions for intermediate non-Hermiticity and test them against QCD-like LGT data from [17]. This further completes the picture, compared to previous approximations [14] ($\beta = 2$) based on a Fredholm determinant expansion [18], and exact results at maximal non-Hermiticity [19] ($\beta = 2, 4$).

2. *Level spacing in the WD class.* We recall here the success of a WS for Hermitian, and its failure for non-Hermitian, WD ensembles. The WD partition function for an $N \times N$ Hermitian matrix H with real, complex or quaternion real entries is given terms of eigenvalues by

$$\mathcal{Z}_{WD}^{(\beta)} = \int dH e^{-\text{Tr} H H^\dagger} \sim \int_{\mathbb{R}} \prod_{j=1}^N d\lambda_j e^{-\lambda_j^2} |\Delta_N(\lambda)|^\beta. \quad (1)$$

The Jacobians of the corresponding ensembles which are called GOE, GUE and GSE ($\beta = 1, 2$ and 4) include the Vandermonde determinant, $\Delta_N(\lambda) \equiv \prod_{k>l}^N (\lambda_k - \lambda_l)$.

The large- N nn spacing in the bulk of the spectrum can be computed approximately from $N = 2$ (WS) by inserting $\delta(|\lambda_1 - \lambda_2| - s)$ in $\mathcal{Z}_{WD}^{(\beta)}$:

$$p_{WS}^{(\beta)}(s) = a_\beta s^\beta \exp[-b_\beta s^2]. \quad (2)$$

The constants a_β, b_β follow from fixing the norm and first moment to unity (see e.g. in [1]). The latter can always be achieved from $\int_0^\infty ds s \hat{p}(s) = m$ by rescaling $p^{(\beta)}(s) = m \hat{p}^{(\beta)}(ms)$. This fixes the scale compared with $N = \infty$.

The exact result $p^{(\beta)}(s)$ is cumbersome, given in terms of an infinite product of eigenvalues of spheroidal functions (e.g. in [2]), the 5th Painlevé transcendent [2], or

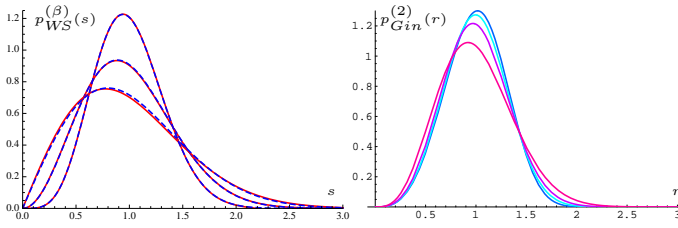


FIG. 1: Left: surmise $p_{WS}^{(\beta)}(s)$ (red) vs exact result (dashed blue) in [20]. Right: $p_{Gin}^{(2)}(r)$ for $N = 2, 3, 4, 20$ (red to blue).

combining a Taylor series with coefficients given by sums over permutations and Dyson's asymptotic expansion in a Padé approximation [20]. This is compared to the surmise Eq. (2) in Fig. 1 left. In Table I we give the root of the integrated square deviation for later comparison,

$$\delta \equiv \left[\int_0^\infty ds (p^{(\beta)}(s) - p_{surmise}^{(\beta)}(s))^2 \right]^{\frac{1}{2}}. \quad (3)$$

The non-Hermitian WD ensembles are defined by dropping the Hermiticity constraint in Eq. (1) left [3]. We only display the complex eigenvalue representation for $\beta = 2$ and 4 and their Jacobians $\mathcal{J}_\beta(z)$ computed in [3]:

$$\mathcal{Z}_{Gin}^{(\beta)} = \int_{\mathbb{C}} \prod_{j=1}^N d^2 z_j e^{-|z_j|^2} \mathcal{J}_\beta(z), \quad (4)$$

$$\mathcal{J}_2(z) = |\Delta_N(z)|^2, \quad \mathcal{J}_4(z) = \Delta_{2N}(z, z^*) \prod_{j=1}^N (z_j - z_j^*).$$

For $\beta = 2$ the spacing is obtained from an $N = 2$ surmise by inserting $\delta(|z_1 - z_2| - r)$ in $\mathcal{Z}_{Gin}^{(2)}$, and putting one eigenvalue at the origin. The exact spacing for any N obtained in [21] uses translational invariance in the bulk

$$\hat{p}_{Gin}^{(2)}(r) = -\frac{\partial E_{Gin}^{(2)}(r)}{\partial r}, \quad E_{Gin}^{(2)}(r) = \prod_{j=1}^{N-1} e^{-r^2} \sum_{k=0}^j \frac{r^{2k}}{k!}. \quad (5)$$

In Fig. 1 right we compare $N = 2$ with increasing N , all curves having norm and first moment 1. Clearly a surmise *does not work* for the $\beta = 2$ Ginibre ensemble ($\delta \approx 0.18$), as previously noted in [21]. For $\beta = 4$ and 1 the spacing is currently unknown.

3. *First eigenvalue in chiral RMT.* The chiral ensembles with real eigenvalues called chGOE, chGUE, and chGSE are defined in terms of $N \times (N + \nu)$ rectangular

	δ_{WS}		$\delta_{\mu=0}^{\nu=0}$	$\delta_{\mu=0}^{\nu=1}$	$\delta_{\mu=0}^{\nu=2}$	$\delta_{\mu=1}^{\nu=0}$	$\delta_{\mu=1}^{\nu=1}$	$\delta_{\mu=1}^{\nu=2}$
GUE	0.04	chGUE	0	3.8	7.7	8.0	12.3	14.8
GSE	0.015	chGSE	1.7	6.1	10.6	1.8	3.3	4.4
GOE	0.16	chGOE	3.6	0	-	-	-	-

TABLE I: Deviation Eq. (3) in units 10^{-3} between approximate $N = 2$ and exact large- N results (δ_{WS} from [20]).

matrices W with real, complex or quaternion real elements without further symmetry restrictions. Switching to positive eigenvalues $\lambda_j \geq 0$ of the Hermitian Wishart (or covariance) matrix WW^\dagger we obtain

$$\mathcal{Z}_\nu^{(\beta)} = \int_0^\infty \prod_{j=1}^N d\lambda_j \lambda_j^d e^{-\lambda_j} |\Delta_N(\lambda)|^\beta, \quad d \equiv \frac{\beta(\nu+1)}{2} - 1. \quad (6)$$

Here N_f massless flavours can be added by shifting $d \rightarrow d + N_f$. The gap probability $E^{(\beta)}(s)$ that the interval $(0, s)$ is void follows by integrating in Eq. (6) from s to ∞ . For $N = 2$ we obtain

$$E_\nu^{(\beta)}(s) \sim \int_0^\infty dx dy [(x+s)(y+x+s)]^d e^{-2(s+x)-y} y^\beta, \quad (7)$$

after shifting variables. The nested integrals can easily be evaluated. Note that $d=0$ for $\beta=2, \nu=0$, and $\beta=1=\nu$. These gap probabilities can be computed exactly for any N , and our surmise gives the *exact* result after rescaling.

To compare with Dirac operator eigenvalues we have to switch variables $\lambda_j \rightarrow y_j^2$, coming in eigenvalue pairs $\pm y_j$, and thus to $s \rightarrow s^2$. The distribution of the first positive Dirac eigenvalue follows: $p_\nu^{(\beta)}(s) = -\partial_s [E_\nu^{(\beta)}(s^2)]$.

We first list all its known $N_f=0$ results in the universal microscopic limit for $\nu \in \mathbb{N}$ in Eqs. (8) - (10): the chGUE for all ν [15, 22], the chGOE for $\nu = 0$ [23] and odd ν [15], and the chGSE for $\nu = 0$ [23] and $\nu > 0$ [24]. For the latter, only a convergent Taylor series is known with coefficients $a_j(\nu)$ given by sums over partitions (see Eq. (8) in [24]), much alike for the WS in the WD class,

$$p_\nu^{(2)}(s) = s e^{-s^2/4} \det_{i,j=1,\dots,\nu} [I_{i-j+2}(s)] / 2, \quad (8)$$

$$p_{\nu=0}^{(1)}(s) = [(2+s) e^{-s^2/8-s/2}] / 4, \quad (9)$$

$$\hat{p}_{\nu=2n+1}^{(1)}(s) \sim s^{(3-\nu)/2} e^{-s^2/8} \text{Pf}_{i,j=-n+\frac{1}{2}, \dots, n-\frac{1}{2}} [(i-j)I_{i+j+3}(s)],$$

$$p_{\nu=0}^{(4)}(s) = (\pi/2)^{\frac{1}{2}} s^{\frac{3}{2}} e^{-s^2/2} I_{3/2}(s), \quad (10)$$

$$\hat{p}_{\nu>0}^{(4)}(s) \sim s^{4\nu+3} e^{-s^2/2} \left(1 + \sum_{j=1}^\infty a_j(\nu) s^j \right).$$

Next, we give examples following our surmise Eq. (7) where $p_\nu^\beta(s)$ is *not* known in elementary form, filling the gaps in Eqs. (8) - (10) for the first two values of $\nu > 0$:

$$\hat{p}_{\nu=2}^{(1)}(s) \sim 3s^3 e^{-\frac{s^2}{8}} + \left(6s^2 - \frac{s^4}{4} \right) e^{-\frac{1}{16}s^2} \sqrt{\pi} \text{Erfc} \left[\frac{s}{4} \right], \quad (11)$$

$$\hat{p}_{\nu=4}^{(1)}(s) \sim \left(s^5 + \frac{s^7}{60} \right) e^{-\frac{1}{8}s^2} + \left(2s^4 - \frac{s^6}{20} \right) e^{-\frac{1}{16}s^2} \sqrt{\pi} \text{Erfc} \left[\frac{s}{4} \right],$$

$$\hat{p}_{\nu=1}^{(4)}(s) \sim s^7 (13440 + 1440s^2 + 60s^4 + s^6) e^{-\frac{1}{2}s^2}, \quad (12)$$

$$\hat{p}_{\nu=2}^{(4)}(s) \sim s^{11} (15482880 + 2150400s^2 + 134400s^4 + 4800s^6 + 100s^8 + s^{10}) e^{-\frac{1}{2}s^2}.$$

The normalisation constants suppressed above easily follow. However, we cannot set the 1st moment to one as

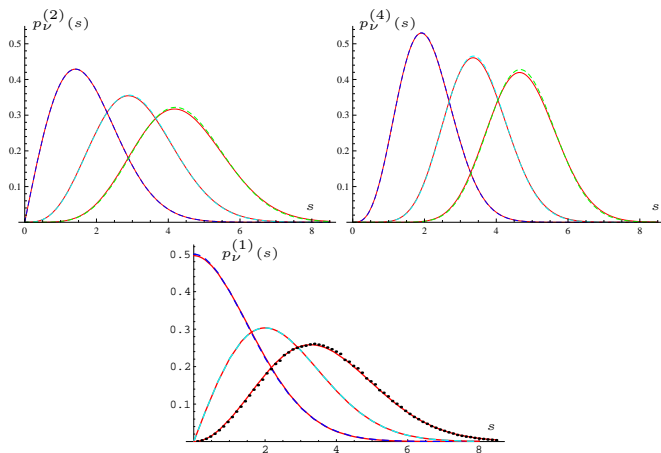


FIG. 2: $p_\nu^{(\beta)}(s)$ with $\nu = 0, 1, 2$ in dashed blue to green for $\beta = 2$ (top left), $\beta = 4$ (top right) and $\beta = 1$ (bottom). The $N = 2$ surmise is in red. Our new result for $\nu = 2$ at $\beta = 1$ is compared to a numerical simulation at $N = 20$ (black dots).

in the WD class. The position of $p_\nu^{(\beta)}(s)$ measures the repulsion by ν exact zero-eigenvalues, containing important information. Thus we fix the $N = 2$ scale by setting the 1st moment equal to the exact one. Without exact ($\beta = 1$, even ν) or concise ($\beta = 4$, $\nu > 0$) results we instead fit to the increasing slope of the known microscopic density $\rho_\nu^{(\beta)}(s)$, being the first term in the Fredholm expansion of the 1st eigenvalue [18] (see also Eq. (18)). In Fig. 2 we compare approximate to exact 1st eigenvalues for small topology $\nu = 0, 1, 2$ and all β . The deviation measured by Eq. (3) in Table I increases with ν , becoming visible only for $\nu = 2$ (see Fig. 2). This has to be compared to the statistical error in data, see e.g. Fig. 5.

Note that in chiral RMT the nn spacing also obeys Eq. (2), but *does not follow* from an $N=2$ surmise [25].

The non-Hermitian chiral ensembles with $\mu \neq 0$ are given in terms of a two-matrix model [11, 26]. We only focus on $\beta = 2, 4$ here, with their complex eigenvalue representations for $N_f = 0$ reading [11, 26]

$$\mathcal{Z}_{\nu\mathbb{C}}^{(\beta)} = \int_{\mathbb{C}} \prod_{j=1}^N d^2 z_j |z_j|^{\beta\nu+2} K_{\frac{\beta\nu}{2}}(a|z_j|^2) e^{b\Re z_j^2} \mathcal{J}_\beta(z^2). \quad (13)$$

The weight $w(z)$ depends on $a \equiv \frac{1+\mu^2}{2\mu^2} > b \equiv \frac{1-\mu^2}{2\mu^2} \geq 0$, with $\mu \in (0, 1]$. The limit $\mu \rightarrow 0$ leads back to real eigenvalues, and at $\mu = 1$ non-Hermiticity is maximal. The definition of a gap probability on \mathbb{C} is not unique [14, 19]. For *radial* ordering it reads

$$E^{(\beta)}(r) \sim \prod_{j=1}^N \int_r^\infty dr_j r_j \int_0^{2\pi} d\theta_j w(z_j) \mathcal{J}_\beta(z). \quad (14)$$

Differentiation yields $\partial_r E^{(\beta)}(r) = \int_0^{2\pi} d\theta p_\nu^{(\beta)}(re^{i\theta})$, the integrated 1st eigenvalue. For $\beta = 2$ (4) the gap proba-

bility is given by a Fredholm determinant (Pfaffian) [19]

$$E^{(2)}(r) \sim \det_{1, \dots, N} \left[\int_{r^2}^\infty dt t^{k+j+\nu-1} K_\nu(at) I_{k+j-2}(bt) \right]. \quad (15)$$

Its matrix elements $A_{jk}^{(\nu)}$ can be computed recursively for any ν by differentiating the following matrix element [19]:

$$A_{11}^{(0)} = \frac{br^2 I_1(br^2) K_0(ar^2) + ar^2 I_0(br^2) K_1(ar^2)}{a^2 - b^2}. \quad (16)$$

This leads to a $\beta \times \beta$ determinant (Pfaffian) representation for our $N = 2$ surmise valid for any μ . At $\mu = 1$ all Fredholm eigenvalues $1 - \lambda_{k=0, \dots, N-1}^{(\beta)}$ are explicitly known [19], providing an exact result for any N as in Eq. (5). It contains incomplete Bessel function series $I_\nu^{[k]}(x)$ truncated at power k ($\equiv 0$ for $k < 0$)

$$(1 - \lambda_k^{(2)}) = \frac{r^{2(2k+\nu+1)}}{2^{2k+\nu} (k+\nu)! k!} K_{\nu+1}(r^2) + r^2 (I_{\nu+2}^{[k-2]}(r^2) K_{\nu+1}(r^2) + I_{\nu+1}^{[k-1]}(r^2) K_{\nu+2}(r^2)). \quad (17)$$

For $\beta = 4$ we have the relation $\lambda_k^{(4)} = \lambda_{2k+1}^{(2)}$ with $\nu \rightarrow 2\nu$ [19]. In Fig. 3 we compare our surmise to this result, truncated at $N = 8$ because of rapid convergence. Here it works better for $\beta = 4$ than $\beta = 2$, in contrast to $\mu = 0$. Due to angular integration only one scale has to be fixed after normalisation, which can be done as in the real case.

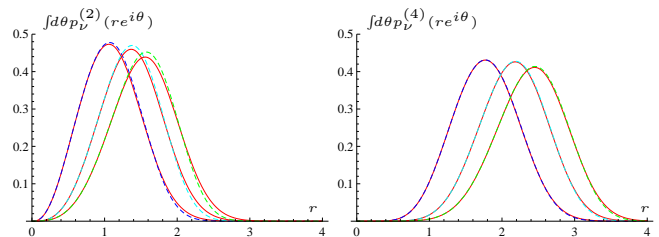


FIG. 3: Integrated 1st eigenvalue at $\mu=1$ for $\nu=0, 1, 2$ (blue to green dashes) vs $N=2$ (red): $\beta=2$ (left) and $\beta=4$ (right).

Next we give a surmise for $p_\nu^{(\beta)}(re^{i\theta})$. In Eq. (14) we skip the integration over θ_1 and differentiate wrt r_1 . For $N = 2$ we obtain an exact Fredholm expansion

$$p_\nu^{(\beta)}(z) = R_{1,\nu}^{(\beta)}(z) - \int_0^{r_1} dt t \int_0^{2\pi} d\varphi R_{2,\nu}^{(\beta)}(z, te^{i\varphi}), \quad (18)$$

with $z = r_1 e^{i\theta_1} = x + iy$. The 1- and 2-point spectral densities are expressed through the kernel of orthogonal Laguerre polynomials of norm h_j (see [11] for details)

$$R_{1,\nu}^{(2)}(z) = K_N^{(2)}(z, z^*) = w(z) \sum_{j=0}^{N-1} \frac{|L_j^{(\nu)}\left(\frac{z^2}{1-\mu^2}\right)|^2}{h_j}, \quad (19)$$

and $R_{2,\nu}^{(2)}(z, u) = R_{1,\nu}^{(2)}(z) R_{1,\nu}^{(2)}(u) - |K_N^{(2)}(z, u^*)|^2$. For $\beta = 4$ we have a Pfaffian of a matrix kernel instead [26]. An

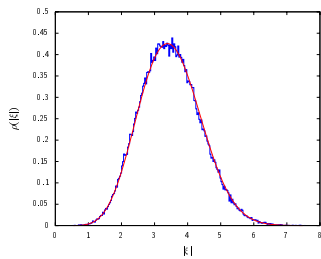


FIG. 4: $\int d\theta p_\nu^{(4)}(re^{i\theta})$ (red) vs Lattice data [17] (blue) with volume $V = 4^4$, gauge coupling 1.3, $\mu_{\text{Lat}} = 0.2$ and mass 20 in Lattice units, using a very large number 10^5 configurations.

example for $p_{\nu=0}^{(4)}(z)$ is shown in Fig. 5 top right. Here two scales have to be fixed: for z we fit to the increase of the known microscopic density in the x -direction, and for rescaling $2N\mu^2 \equiv \alpha^2$ to its decrease in the y -direction. Since $\alpha \leq 2$ for $N = 2$, we conclude that at large- N for $\alpha > 2$ $p_\nu^{(\beta)}(z)$ must become symmetric wrt rotation ($\beta = 2$) or reflections wrt the bisector of each quadrant ($\beta = 4$). We have checked this, as well as distributions for $0 < \mu < 1$ by generating ensembles of large random matrices.

4. *Lattice data.* In [17] two-colour QCD was compared to the $\beta = 4$ microscopic spectral density in the complex plane from chiral RMT [26]. We use the same data here but with higher statistics, and refer to [17] for all simulation details. Because unimproved staggered fermions are used we are in the $\beta = 4$ class at $\nu = 0$. Our $N_f = 2$ data are effectively quenched for the smallest eigenvalues due to a large mass. In Fig. 4 we compare to the 1st integrated eigenvalue, with $\alpha = 1.352$ being close to maximal non-Hermiticity. No further fits compared to [17] are made. In Fig. 5 we compare LGT data at intermediate $\mu_{\text{Lat}} = 0.1$ to the angle-dependent surmise Eq. (18) by taking cuts. Here the two scales are fitted to the data, finding an excellent agreement for $\alpha = 0.65$.

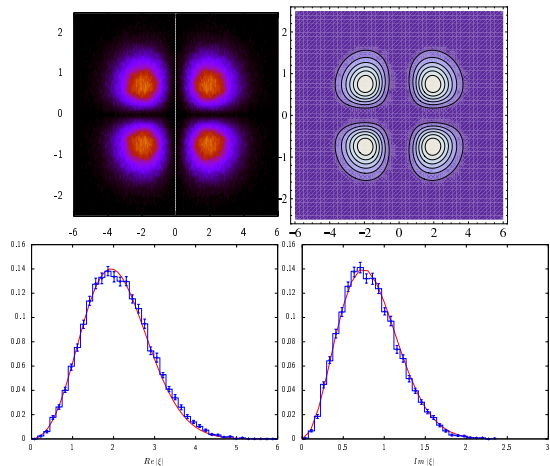


FIG. 5: Top: contour plots for Lattice data as in Fig. 4 but with $\mu_{\text{Lat}} = 0.1$ (left) vs surmise Eq. (18) (right). Bottom: cuts through a single peak in x - (left) and y -direction (right).

An alternative to Eq. (18) is the truncated Fredholm expansion in the microscopic large- N limit [18] which was successfully applied to the $\beta = 2$ class [14]. However, integrals of higher order terms rapidly become cumbersome.

5. *Conclusions.* Conceptually it is possible within chiral RMT to approximate the 1st eigenvalue distribution using a $2 \times (2 + \nu)$ matrix calculation, for both real and complex eigenvalues. It is remarkable that this surmise works and captures the repulsion of ν zero-eigenvalues. We derived new compact expressions for $\beta = 1$ and 4 with real eigenvalues for $\nu > 0$. Second, we have shown that our surmise for $\beta = 4$ successfully describes $SU(2)$ Lattice data, in an intermediate regime for $\mu \neq 0$ where no results were previously known. It would be very interesting to extend our results to the $\beta = 1$ non-Hermitian chiral class, having both real and complex eigenvalues.

Support by ENRAGE MRTN-CT-2004-005616 (G.A., E.B.), EPSRC grant EP/D031613/1 (G.A., L.S.) and DFG grant JA483/22-1 (E.B.) is acknowledged.

-
- [1] T. Guhr, A. Müller-Groeling, H.A. Weidenmüller, Phys. Rep. **299** (1998) 190.
 - [2] M.L. Mehta, *Random Matrices*, Academic Press, Third Edition, London 2004.
 - [3] J. Ginibre, J. Math. Phys. **6** (1965) 440.
 - [4] Y.V. Fyodorov, H.J. Sommers, J. Phys. **A36** (2003) 3303.
 - [5] H. Markum, R. Pullirsch, T. Wettig, Phys. Rev. Lett. **83** (1999) 484.
 - [6] E.V. Shuryak, J.J.M. Verbaarschot, Nucl. Phys. **A560** (1993) 306.
 - [7] M. Stephanov, Phys. Rev. Lett. **76** (1996) 4472.
 - [8] R.G. Edwards, U.M. Heller, J.E. Kiskis, R. Narayanan, Phys. Rev. Lett. **82** (1999) 4188.
 - [9] J. Bloch, T. Wettig, Phys. Rev. Lett. **97** (2006) 012003.
 - [10] S. Ejiri, PoS (LATTICE 2008) 002.
 - [11] J.C. Osborn, Phys. Rev. Lett. **93** (2004) 222001.
 - [12] G. Akemann, J.C. Osborn, K. Splittorff, J.J.M. Verbaarschot Nucl. Phys. **B712** (2005) 287.
 - [13] K. Splittorff, J.J.M. Verbaarschot, Phys. Rev. Lett. **98** (2007) 031601; Phys. Rev. **D75** (2007) 116003.
 - [14] G. Akemann, J. Bloch, L. Shifrin, T. Wettig, Phys. Rev. Lett. **100** (2008) 032002.
 - [15] P.H. Damgaard, S.M. Nishigaki, Phys. Rev. **D63** (2001) 045012.
 - [16] P.V. Buividovich, E.V. Luschevskaya, M.I. Polikarpov, Phys. Rev. **D78** (2008) 074505.
 - [17] G. Akemann, E. Bittner, Phys. Rev. Lett. **96** (2006) 222002.
 - [18] G. Akemann, P.H. Damgaard, Phys. Lett. **B583** (2004) 199.
 - [19] G. Akemann, M.J. Phillips, L. Shifrin, J. Math. Phys. **50** (2009) 063504.
 - [20] B. Dietz, F. Haake, Z. Phys. **B80** (1990) 153.
 - [21] R. Grobe, F. Haake, H.J. Sommers, Phys. Rev. Lett. **61** (1988) 1899.
 - [22] T. Wilke, T. Guhr, T. Wettig, Phys. Rev. **D57** (1998) 6486; S.M. Nishigaki, P.H. Damgaard, T. Wettig, Phys. Rev. **D58** (1998) 087704.
 - [23] P.J. Forrester, Nucl. Phys. **B402** (1993) 709.

- [24] M.E. Berbenni-Bitsch, S. Meyer, T. Wettig, Phys. Rev. **D58** (1998) 071502.
- [25] A.Y. Abul-Magd, G. Akemann, P. Vivo, J. Phys. **A42** (2009) 175207.
- [26] G. Akemann, Nucl. Phys. **B730** (2005) 253.